ACS APPLIED MATERIALS & INTERFACES

Letter

www.acsami.org

Colorimetric Sensor Array Based on Gold Nanoparticles and Amino Acids for Identification of Toxic Metal Ions in Water

Gulsu Sener,[†,‡] Lokman Uzun,[†] and Adil Denizli*[,†]

[†]Department of Chemistry, Faculty of Science , and [‡]Nanotechnology and Nanomedicine Division, Institute of Science, Hacettepe University, Ankara, Turkey

Supporting Information

ABSTRACT: A facile colorimetric sensor array for detection of multiple toxic heavy metal ions (Hg^{2+}, Cd^{2+}, Fe^{3+}, Pb^{2+}, Al^{3+}, Cu^{2+}, and Cr^{3+}) in water is demonstrated using 11-mercaptoundecanoic acid (MUA)-capped gold nanoparticles (AuNPs) and five amino acids (lysine, cysteine, histidine, tyrosine, and arginine). The presence of amino acids (which have functional groups that can form complexes with metal ions and MUA) regulates the aggregation of MUA-capped particles; it can either enhance or diminish the particle aggregation. The combinatorial colorimetric response of all channels of the sensor array (i.e., color change in each of AuNP and amino acid couples) enables naked-eye discrimination of all of the metal ions tested in this study with excellent selectivity.

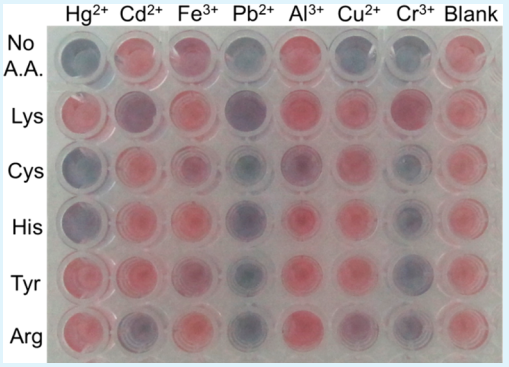

KEYWORDS: *toxic metal ions, gold nanoparticles, colorimetric assays, sensor array, environmental monitoring*

Toxic heavy metal ions (e.g., Hg^{2+}, Pb^{2+}, Cd^{2+}) can cause serious environmental and health problems at even very low concentrations. Humans and other living organisms can be exposed to the toxic metal ions through water, air, soil, and food.[1,2] Therefore, reliable detection of toxic metal ion levels in these sources is important for improving the public health and controlling the environmental pollution. Common methods for the detection of metal ions are mostly spectroscopy based techniques such as atomic absorption, ion-coupled-plasma, inductively coupled plasma emission, and inductively coupled plasma mass spectroscopies.[3−5] However, these methods require intense technical training because of their complicated procedures, and they are expensive and time-consuming.

Recently, metal nanoparticle (mostly gold or silver) based colorimetric assays for toxic metal ion detection have been emerged as a simple and low-cost alternative of spectroscopy based methods.[6−13] These assays are based on controlled aggregation of surface modified (with aptamers, peptides etc.) metal nanoparticles in the presence of metal ions. Aggregation of metal nanoparticles in the presence of analyte ions changes the color of nanoparticles solution. Therefore, rapid and sensitive detection of metal ions without the need of any equipment (i.e., naked eye observation of color changes) or using a simple UV−vis absorption spectrophotometer can be achieved. Although many successful colorimetric probes have been reported for detection of single specific metal ions; colorimetric sensor arrays that are capable of detection of multiple metal ions are very rare.[3,14,15] One example of such colorimetric assays is reported by Kim et al.[3] which uses simple MUA-capped AuNPs for simultaneous detection of Hg^{2+}, Pb^{2+}, Cd^{2+} ions through ion-templated chelation process between these divalent metal ions and carboxyl groups of MUA molecules. However, the assay lacks of selectivity between the metal ions. Same problem is applicable for the other multiple metal ion colorimetric assays.

In this paper, we describe a colorimetric sensor array that is capable of discrimination of seven metal ions (Hg^{2+}, Cd^{2+}, Fe^{3+}, Pb^{2+}, Al^{3+}, Cu^{2+}, and Cr^{3+}) simultaneously with excellent selectivity. The colorimetric assay is based on metal ion induced aggregation of MUA-capped AuNPs in the presence of different amino acids (lysine, cysteine, histidine, tyrosine, and arginine). Amino acids were used because they can bind AuNPs through their amino groups and also can form complexes with metal ions through their carboxyl and amino groups.[3,10,16,17] In addition, their side chains may also contain functional groups that have affinity to both AuNPs and metal ions; for example mercapto group of cysteine or second amino group of lysine. Accordingly, use of amino acids provides the selectivity by interacting AuNPs and metal ions with many different pathways. Each of the amino acids and MUA-capped AuNPs forms a distinct sensor element of the colorimetric array. We observed that presence of amino acids can either enhance or diminish the metal induced aggregation. Aggregation of AuNPs changes the color of nanoparticle solution from red to purple or blue.[7] Therefore, by analyzing the combinatorial colorimetric response (e.g., using hierarchical cluster analysis or simply by

Received: June 4, 2014
Accepted: October 20, 2014
Published: October 20, 2014

   dx.doi.org/10.1021/am5071283 | ACS Appl. Mater. Interfaces 2014, 6, 18395−18400

naked-eye) of the each sensor element, it is possible to discriminate all of the seven metal ions tested in this study.

The binding ability of amino acids onto the surface of MUA-capped AuNPs were investigated using Raman spectroscopy and zeta potential measurements. In order to obtain the Raman spectra, we incubated the AuNPs with amino acids for approximately 15 min and washed the AuNPs several times in order to remove the unbound amino acids. Then, we dried the solutions onto the glass substrates and collected Raman spectra of AuNPs. The Raman peaks corresponding to the organic groups[18] (e.g., $-CH_2-$ and $-COOH$) increased significantly after interacting the AuNPs with amino acids (see the Supporting Information, Figure S1) indicating the amino acid binding to the AuNP surface. In addition, zeta potential measurements showed that after amino acid treatment zeta potential of the AuNPs become more negative which also points out the amino acid binding to the surface (see the Supporting Information, Table S1). Amino acids can easily bind onto the AuNP surfaces through their amino groups.[19]

In the colorimetric assay, many different interactions between AuNPs, amino acids, and metal ions are possible (Scheme 1). The results of Raman spectroscopy and Zeta potential measurements indicated that amino acids can bind to the MUA-capped AuNP surfaces and form mixed ligand surfaces. Accordingly, we considered that some of the amino acids attached to the surface of AuNPs and some are free in the solution and we proposed the following mechanisms. First of all, there may be no interaction with AuNPs and they are not aggregated (Scheme 1a). Note that in this scenario, there may be interaction between amino acids and metal ions but in the both cases AuNPs well-dispersed in the solution. In the second mechanism, metal ions can induce the aggregation of AuNPs (Scheme 1b) and result in a color change. Here, presence of amino acids has no effect on the colorimetric response. In the third scenario, amino acids can interact with metal ions that normally aggregate AuNPs and prevent the aggregation (Scheme 1c). Lastly, metal ions and amino acids can co-contribute the aggregation of AuNPs (Scheme 1d). Also, mechanisms related with amino acid induced aggregation of AuNPs can be proposed. However, in our experimental conditions, amino acids did not cause aggregation of AuNPs in the absence of metal ions; therefore mechanisms related with amino acid induced aggregation are not applicable for our colorimetric array. In addition, structure of MUA-capped AuNPs and some possible interactions between functional groups and metal ions were demonstrated in Figure S2 (see the Supporting Information).

Scheme 1. Schematic Representation of Proposed Metal Ions, Amino Acids, and AuNP Interactions: (a) No Interaction, (b) Metal Ions Induce the Aggregation of AuNPs, (c) Amino Acids Interact with Metal Ions and Prevent Aggregation of AuNPs; and (d) Metal Ions and Amino Acids Co-Contribute the Aggregation of AuNPs

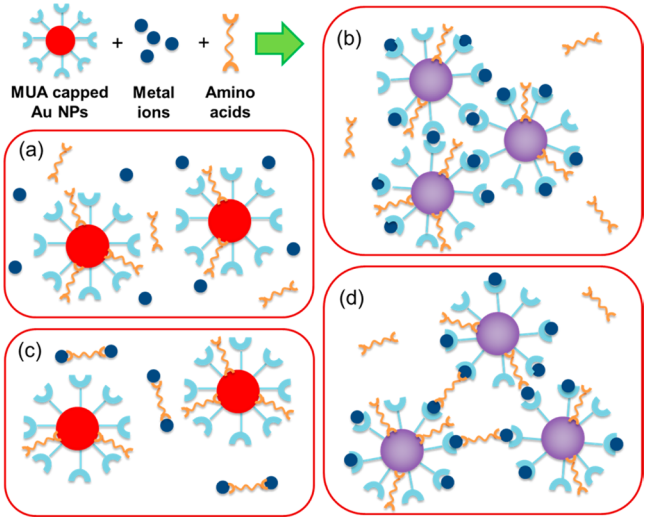

Figure 1 shows the response (i.e., extinction at 625 nm/525 nm; $Ex_{625/525}$) of the colorimetric assay against seven metal ions (Hg^{2+}, Cd^{2+}, Fe^{3+}, Pb^{2+}, Al^{3+}, Cu^{2+}, and Cr^{3+}) at different concentrations between 2 and 50 μM. The representative UV–vis spectra of AuNPs in the presence of Cd^{2+} (20 μM) and lysine are given in Figure S3 (see the Supporting Information). There was only a slight change in the UV–vis spectra of AuNPs in the presence only Cd^{2+} and $Ex_{625/525}$ value is almost same with the blank control. In the presence of both lysine and Cd^{2+}, on the other hand, absorption at around 625 nm increased, which indicates the aggregation of AuNPs[6] and accordingly colorimetric response is increased significantly which can be also observed from Figure 1. The aggregation of AuNPs was also investigated using TEM (see the Supporting Information, Figure S4). In the absence of lysine and Cd^{2+} AuNPs were well-separated and dispersed onto the TEM grid (see Supporting Information, Figure S4a); however in the presence of lysine and Cd^{2+} AuNPs aggregated and formed large clusters (see the Supporting Information, Figure S4b).

The average particles size of AuNPs was calculated to be 29.8 ± 5.3 nm from TEM images (see the Supporting Information, Figure S4a). AuNP concentration in the assay is 0.1 nM (which was calculated according to a previous report using the TEM size of particles[20]) and amino acid concentration is 50 μM for cysteine and 200 μM for other amino acids. Amino acid concentrations were selected to ensure no aggregation of AuNPs in the absence of metal ions (see the Supporting Information, Figures S5 and S6). We studied the effect of amino acid concentration on the aggregation of AuNPs in the concentration range of 0 to 500 μM. It was observed that expect cysteine none of the amino acids cause significant aggregation of AuNPs; Ex_{625}/Ex_{525} values remained almost unaffected. For cysteine, on the other hand, a concentration-dependent aggregation and increase in Ex_{625}/Ex_{525} value was observed. Nevertheless, up to a concentration of 100 μM cysteine did not cause significant aggregation. Accordingly, we selected the amino acid concentrations as 50 μM for cysteine and 200 μM for other amino acids (see the Supporting Information, Figure S5). In addition, we studied the stability of the amino acid (above selected amino acid concentrations were used) added AuNP solutions for 1 h. No aggregation was observed even after 1 h (see the Supporting Information, Figure S6). In addition, to investigate effect of salinity on the response of AuNPs, we added different amounts of phosphate buffered saline (PBS) (pH 7.4, 10 mM) on to the MUA-capped AuNPs. It was observed that above the final PBS concentration of 2 mM AuNPs aggregated and $Ex_{625/525}$ values gradually increases with the increasing PBS solution (see the Supporting Information, Figure S7). Nevertheless, the assay can be used in mild salinity conditions. Also, it is important to note that MUA-capped AuNPs were stable at least for two months at 4 °C.

dx.doi.org/10.1021/am5071283 | ACS Appl. Mater. Interfaces 2014, 6, 18395–18400

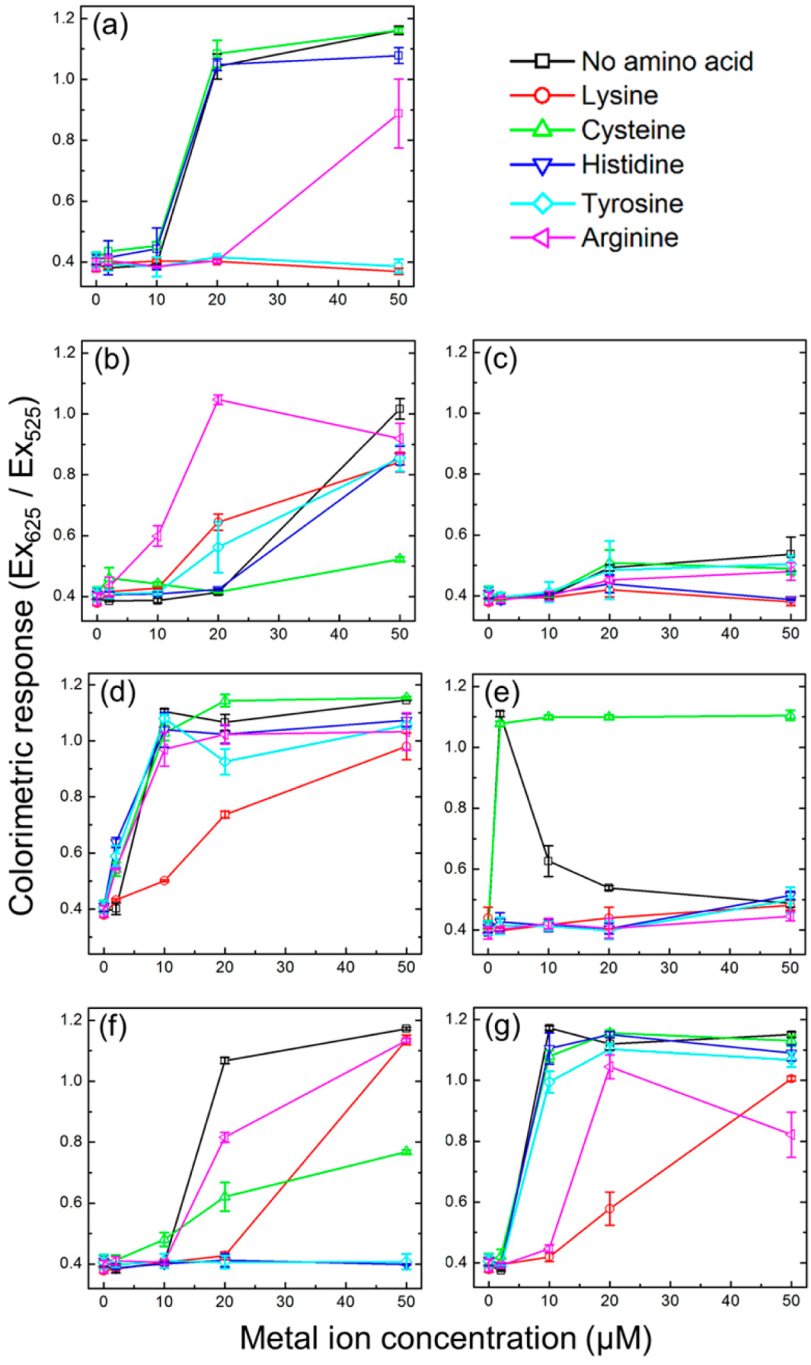

Figure 1. Effect of metal ion concentration (0−50 μM) on the response (Ex_{625}/Ex_{525}) of the colorimetric sensor array. (a) Hg^{2+}, (b) Cd^{2+}, (c) Fe^{3+}, (d) Pb^{2+}, (e) Al^{3+}, (f) Cu^{2+}, and (g) Cr^{3+}.

All proposed mechanisms of AuNP aggregation can be observed from Figure 1. For example, in the presence of lysine and 10 μM of Hg^{2+}, the response of the assay is similar to the blank (i.e., only AuNPs) which indicates that MUA-capped AuNPs are not aggregated (proposed mechanism a). In the presence of 20 μM of Cr^{3+}, AuNPs aggregate independent from the presence of cysteine, which can be given as an example of mechanism b. In the presence of 20 μM Cu^{2+}, AuNPs aggregate; however, when tyrosine is in the solution, no aggregation is observed and the response of the assay remains unchanged (proposed mechanism c). Lastly, in the absence of arginine 10 μM Cd^{2+} does not interact with MUA-capped AuNPs, whereas the aggregation is observed if arginine was added (proposed mechanism d).

The colorimetric sensor array enables naked eye discrimination of the seven metal ions. For instance, Figure 2a shows a representative photograph of the colorimetric array response against 20 μM of metal ions. As it can be clearly seen from the photograph each of the metal ions produce different color pattern. We observed that some metal ions produce more colorimetric response (i.e., changing the original red color of AuNPs in more channels) than others. For example, Pb^{2+} and Cr^{3+} promoted aggregation at five of the six channels; on the other hand addition of Al^{3+} produced slight color change at only one of the channels. In addition, we tested nine more

dx.doi.org/10.1021/am5071283 | ACS Appl. Mater. Interfaces 2014, 6, 18395−18400

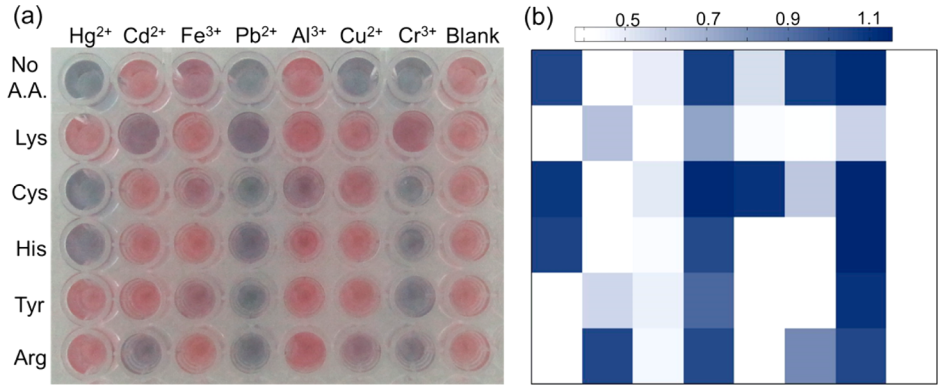

Figure 2. (a) Representative photograph of the colorimetric sensor array response against 20 μM of metal ions. (b) Blue-scale representation of the colorimetric sensor array response. White corresponds to no aggregation and blue corresponds to aggregation of AuNPs.

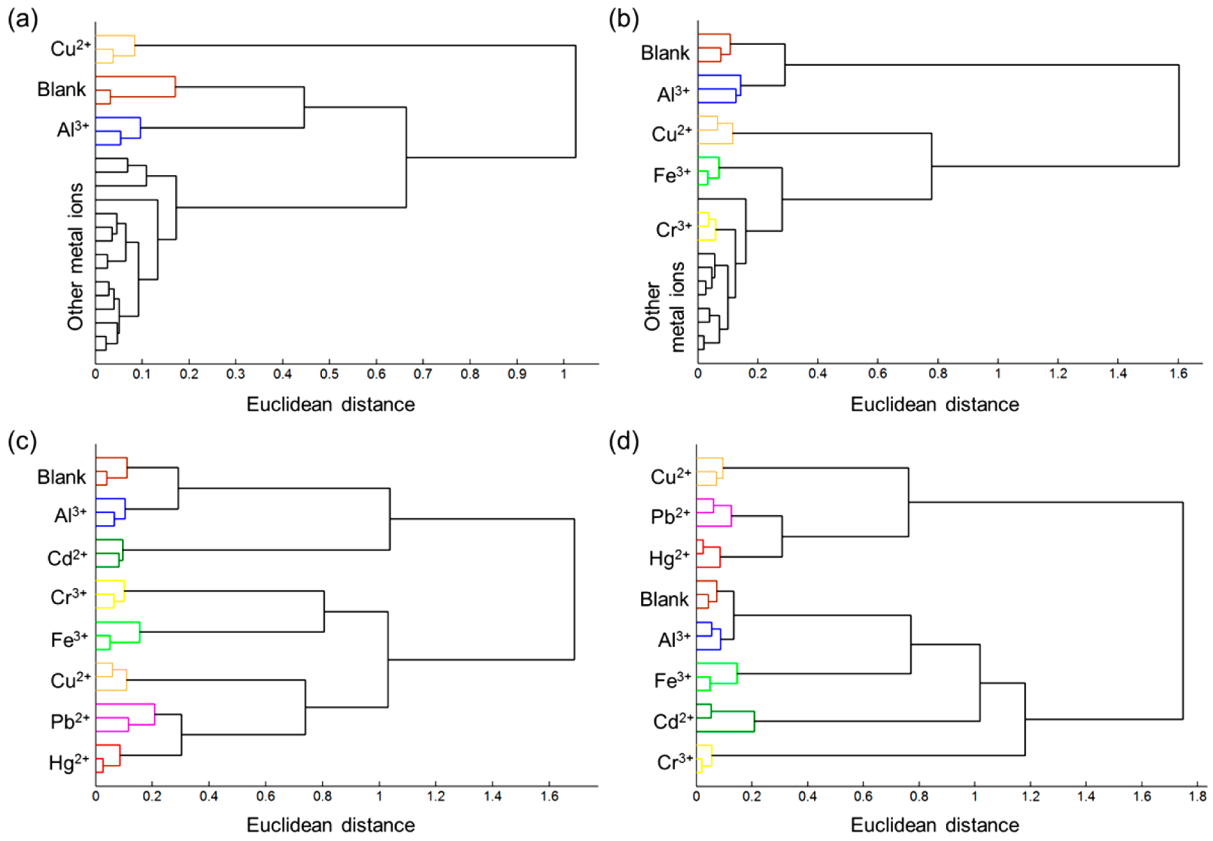

Figure 3. Hierarchical cluster analysis of colorimetric sensor array of seven different metal ions at different metal ion concentrations: at (a) 2, (b) 10, (c) 20, and (d) 50 μM.

metal ions (Ag^{+}, Ca^{2+}, Zn^{2+}, Co^{2+}, Ni^{2+}, Sr^{2+}, K^{+}, Na^{+}, Fe^{2+}) and their mixtures with the assay. We observed that none of these metal ions produce significant color change (i.e., response) in any channel (see the Supporting Information, Figure S8). It is important to note that, the response of the assay against the same metal ion with different valence numbers is different. For example, for iron ions; Fe^{3+} produced colorimetric response in three channels of the assay (Figure 2), whereas Fe^{2+} did not produce any response (see the Supporting Information, Figure S8). This result indicate that the colorimetric assay can be also used for discriminate the metal ions with different valence numbers.

The different affinity of the metal ions with the colorimetric sensor array can be explained with the difference in chelate formation capability of metal ions with carboxyl groups of MUA molecules and functional groups (amino, carboxyl, thiol etc.) of amino acids.[21] The colorimetric response of the array against metal ions in Figure 2a can be also expressed as color mapping using simple software for clearer representation. Figure 2b shows blue-scale color map of averaged response from three separate measurements of the array against 20 μM of each metal ion. The color map demonstrates the excellent discrimination among all tested metal ions.

To demonstrate reproducibility of the colorimetric sensor array response, a hierarchical cluster analysis (HCA) was performed using the Euclidean algorithm (see the Supporting Information for details).[22,23] Figure 3 shows the results of HCA analysis of the array response against metal ions at different

concentrations for three separate experiments. The dendrogram demonstrates that at high metal ion concentrations (20 and 50 μM) all of the metal ions can be successfully identified without a mistake for all of the three separate experiments indicating the good reproducibility of the colorimetric sensor array. At low concentrations (2 and 10 μM), on the other hand, response of some metal ions interfere with each other; at 2 μM, only 2 of 7 metal ions, and at 10 μM, 4 of 7 metal ions can be identified. In addition, we performed HCA analysis for the averaged response of all concentrations between 2 μM and 50 μM (using the data represented in Figure 1). There is good discrimination between most of the tested solutions especially at high metal ion concentrations (see the Supporting Information, Figure S9). At low concentrations (2 and 10 μM) of weakly responsive metal ions (e.g., Hg^{2+}, Fe^{2+} and Cu^{2+}), discrimination (e.g., difference from the response of blank) is not very clear. Nevertheless, the colorimetric sensor array can identify most of the cases depending on the metal ion concentration and responsivity.

Lastly, we tested binary and ternary mixtures of three metal ions (Hg^{2+}, Cd^{2+}, Fe^{3+}) with the colorimetric assay. The assay successfully discriminate the all combinations (Figure 4). One

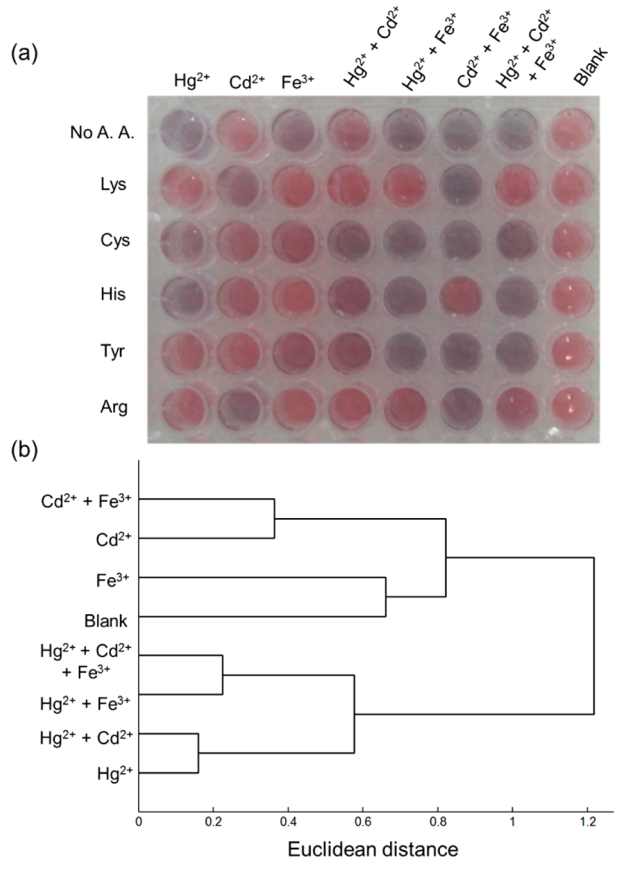

Figure 4. Colorimetric response of the colorimetric array against Hg^{2+}, Cd2^{+}, and Fe^{3+} ions (20 M) and their binary and ternary mixtures. (a) Representative photograph and (b) hierarchical cluster analysis.

can expect that in the presence of two metal ions the response of the colorimetric assay should be the addition of their responses with the assay. Although this is true for most of the cases, we observed that for some cases it is more complicated (Figure 4a). For example, when there was only Cd^{2+} present in the assay, color change in the lysine channel was observed. Interestingly, presence of Hg^{2+} prevents the colorimetric response of Cd^{2+} in this channel. Whereas, presence of Fe^{3+} has no effect on the colorimetric response of Cd^{2+} in the lysine channel.

In conclusion, we have demonstrated a colorimetric sensor array that can simultaneously detect and identify several heavy metal ions (Hg^{2+}, Cd^{2+}, Fe^{3+}, Pb^{2+}, Al^{3+}, Cu^{2+}, and Cr^{3+}) in aqueous media, to our knowledge for the first time. The colorimetric sensor array utilizes MUA-capped AuNPs and amino acids. In the absence of amino acids MUA-capped AuNPs are aggregated by most of the studied metal ions. The presence of amino acids (lysine, cysteine, histidine, tyrosine, and arginine) either enhances or prevents the aggregation of the MUA-capped AuNPs. The possible mechanisms of aggregation/colloidal stability were discussed. By analyzing the combinatorial response of the array components (i.e., each AuNP and amino acid couple), all of the tested metal ions can be discriminated in a broad concentration range. This concentration range is highly dependent to the responsivity (i.e., ability to induce aggregation of AuNPs) of the metal ions. For example, highly responsive Pb^{2+} ions can be identified between 2 and 50 μM; on the other hand, weakly responsive Fe^{3+} ions can be identified at the concentrations above 10 μM (see the Supporting Information, Figure S9). In addition, the response of the colorimetric sensor array is highly reproducible; it discriminated all tested metal ions for three separate experiments without a mistake at the metal ion concentration of 20 μM. Although the reached sensitivity (low μM level) using MUA-capped AuNPs does not satisfy the needed detection limit (around low nM level) for real-world applications, it is possible to design colorimetric arrays for metal ion detection from real samples using simply metal nanoparticles that are capped with different ligands (peptides, aptamers, citrate, etc.) according to the general method described in this study. In addition, we believe that the introduced straightforward colorimetric detection method can be easily adopted to other metal ions and as well as other chemical sensing platforms including proteins, peptides sugars, and organic contaminants.

■ ASSOCIATED CONTENT

Supporting Information

Experimental details, details of HCA analysis, and additional data. This material is available free of charge via the Internet at http://pubs.acs.org.

■ AUTHOR INFORMATION

Corresponding Author

*E-mail: denizli@hacettepe.edu.tr. Tel: +90 312 297 7983. Fax: +90 312 299 2163.

Notes

The authors declare no competing financial interest.

■ REFERENCES

(1) Clarkson, T. W.; Magos, L.; Myers, G. J. The Toxicology of Mercury: Current Exposures and Clinical Manifestations. *N. Engl. J. Med.* **2003**, *349*, 1731−1737.

(2) Kang, T.; Yoo, S. M.; Kang, M.; Lee, H.; Kim, H.; Lee, S. Y.; Kim, B. Single-Step Multiplex Detection of Toxic Metal Ions by Au Nanowires-on-Chip Sensor Using Reporter Elimination. *Lab Chip* **2012**, *12*, 3077−3081.

(3) Kim, Y.; Johnson, R. C.; Hupp, J. T. Gold Nanoparticle-Based Sensing of "Spectroscopically Silent" Heavy Metal Ions. *Nano Lett.* **2001**, *1*, 165−167.

(4) Udhayakumari, D.; Suganya, S.; Velmathi, S.; MubarakAli, D. Naked Eye Sensing of Toxic Metal Ions In Aqueous Medium Using Thiophene-Based Ligands and Its Application in Living Cells. *J. Mol. Recognit.* **2014**, *27*, 151−159.
(5) Bontidean, I.; Berggren, C.; Johansson, G.; Csöregi, E.; Mattiasson, B.; Lloyd, J. R.; Jakeman, K. J.; Brown, N. L. Detection of Heavy Metal Ions at Femtomolar Levels Using Protein-Based Biosensors. *Anal. Chem.* **1998**, *70*, 4162−4169.
(6) Sener, G.; Uzun, L.; Denizli, A. Lysine-Promoted Colorimetric Response of Gold Nanoparticles: A Simple Assay for Ultrasensitive Mercury(II) Detection. *Anal. Chem.* **2014**, *86*, 514−520.
(7) Saha, K.; Agasti, S. S.; Kim, C.; Li, X.; Rotello, V. M. Gold Nanoparticles in Chemical and Biological Sensing. *Chem. Rev.* **2012**, *112*, 2739−2779.
(8) Lou, T.; Chen, Z.; Wang, Y.; Chen, L. Blue-to-Red Colorimetric Sensing Strategy for Hg^{2+} and Ag^{+} via Redox-Regulated Surface Chemistry of Gold Nanoparticles. *ACS Appl. Mater. Interfaces* **2011**, *3*, 1568−1573.
(9) Zheng, Q.; Han, C.; Li, H. Selective and Efficient Magnetic Separation of Pb^{2+} via Gold Nanoparticle-Based Visual Binding Enrichment. *Chem. Commun.* **2010**, *46*, 7337−7339.
(10) Chai, F.; Wang, C.; Wang, T.; Li, L.; Su, Z. Colorimetric Detection of Pb^{2+} Using Glutathione Functionalized Gold Nanoparticles. *ACS Appl. Mater. Interfaces* **2010**, *2*, 1466−1470.
(11) Lee, J. S.; Han, M. S.; Mirkin, C. A. Colorimetric Detection of Mercuric Ion (Hg^{2+}) in Aqueous Media Using DNA-Functionalized Gold Nanoparticles. *Angew. Chem., Int. Ed.* **2007**, *46*, 4093−4096.
(12) Wu, Y.; Zhan, S.; Wang, F.; He, L.; Zhi, W.; Zhou, P. Cationic Polymers and Aptamers Mediated Aggregation of Gold Nanoparticles for The Colorimetric Detection of Arsenic(III) in Aqueous Solution. *Chem. Commun.* **2012**, *48*, 4459−4461.
(13) Dang, Y.-Q.; Li, H.-W.; Wang, B.; Li, L.; Wu, Y. Selective Detection of Trace Cr^{3+} in Aqueous Solution by Using 5,5′-Dithiobis (2-Nitrobenzoic acid)-Modified Gold Nanoparticles. *ACS Appl. Mater. Interfaces* **2009**, *1*, 1533−1538.
(14) Slocik, J. M.; Zabinski, J. S., Jr; Phillips, D. M.; Naik, R. R. Colorimetric Response of Peptide-Functionalized Gold Nanoparticles to Metal Ions. *Small* **2008**, *4*, 548−551.
(15) Zhang, G.; Lin, W.; Yang, W.; Lin, Z.; Guo, L.; Qiu, B.; Chen, G. Logic Gates for Multiplexed Analysis of Hg^{2+} and Ag^{+}. *Analyst* **2012**, *137*, 2687−2691.
(16) Cush, R.; Cronin, J. M.; Stewart, W. J.; Maule, C. H.; Molloy, J.; Goddard, N. J. The Resonant Mirror: A Novel Optical Biosensor for Direct Sensing of Biomolecular Interactions Part I: Principle of Operation and Associated Instrumentation. *Biosens. Bioelectron.* **1993**, *8*, 347−354.
(17) Promnimit, S.; Bera, T.; Baruah, S.; Dutta, J. Chitosan Capped Colloidal Gold Nanoparticles for Sensing Zinc Ions in Water. *J. Nano Res.* **2011**, *16*, 55−61.
(18) Ma, C.; Harris, J. M. Surface-Enhanced Raman Scattering Study of the Kinetics of Self- Assembly of Carboxylate-Terminated n-Alkanethiols on Silver. *Langmuir* **2012**, *28*, 2628−2636.
(19) Zakaria, H. M.; Shah, A.; Konieczny, M.; Hoffmann, J. A.; Nijdam, A. J.; Reeves, M. E. Small Molecule- and Amino Acid-Induced Aggregation of Gold Nanoparticles. *Langmuir* **2013**, *29*, 7661−7673.
(20) Haiss, W.; Thanh, N. T. K.; Aveyard, J.; Fernig, D. G. Determination of Size and Concentration of Gold Nanoparticles from UV−Vis Spectra. *Anal. Chem.* **2007**, *79*, 4215−4221.
(21) Rulisek, L.; Havlas, Z. Theoretical Studies of Metal Ion Selectivity. 1. DFT Calculations of Interaction Energies of Amino Acid Side Chains with Selected Transition Metal Ions (Co^{2+}, Ni^{2+}, Cu^{2+}, Zn^{2+}, Cd^{2+}, and Hg^{2+}). *J. Am. Chem. Soc.* **2000**, *122*, 10428−10439.
(22) Musto, C. J.; Lim, S. H.; Suslick, K. S. Colorimetric Detection and Identification of Natural and Artificial Sweeteners. *Anal. Chem.* **2009**, *81*, 6526−6533.
(23) Yildirim, A.; Ozturk, F. E.; Bayindir, M. Smelling in Chemically Complex Environments: An Optofluidic Bragg Fiber Array for Differentiation of Methanol Adulterated Beverages. *Anal. Chem.* **2013**, *85*, 6384−6391.